Rake receiver improvement for residual interference cancellation in UWB context

Anne-Laure Deleuze and Christophe Le Martret
Thalès Corp., Colombes, France
anne-laure.deleuze@enst.fr
christophe.le_martret@fr.thalesgroup.com

Philippe Ciblat
ENST, Paris, France
philippe.ciblat@enst.fr

***Abstract*—In the context of PAM Time-Hopping/Direct Sequence Impulse Radio Ultra Wide Band (IR-UWB), a residual interference occurs at the output of the Rake Receiver when realistic multipath propagation channel is considered even if a large guard-time interval is used. As a consequence, the performance is limited and exhibits BER floor. In this paper, we explicitly explains what causes such a residual interference. Secondly, we propose a simple way to modify the Rake receiver in order to totally remove this residual interference. The results are illustrated by simulations that validate the proposed method.**

I. Introduction

For several years, the Impulse Radio Ultra Wide Band (IR-UWB) based communication has received a lot of interest, especially for short-range and medium data rate communication schemes (see, *e.g.*, standard IEEE.15.4a). For these applications, the main ”signal processing” challenge is to design a low-complexity and low-cost terminal.

Unfortunately, the propagation channel introduces multi-path component, and Inter-Symbol Interference (ISI) usually occurs at the receiver. To combat this kind of interference, one can i) apply equalization-like technique carried out after the standard Rake receiver (see [3], [4], [1], [2], [5]), ii) modify the weights of each finger of the Rake receiver (see [8]), iii) or insert a time-guard interval at each frame (see [10], [11], [7]).

The third solution obviously is the simplest one and the most spread in practical devices. Nevertheless, even if the guard time is large enough, a residual interference may remain and degrade the performance [6], [9]. Indeed, when the path delay is less than the pulse duration, pulses associated with the same symbol can overlap and create the ”residual interference”, also called, ”cross modulation interference”.

A lot of recent works have focused on the Inter-Symbol Interference mitigation whereas the elimination of the residual interference is seldom treated.

In this paper, we propose a slight modification of the Rake Receiver in order to cancel the residual interference in the context of the PAM (Time-Hopping or Direct Sequence) IR-UWB [1]

[1]This paper has been partially produced as part of the NEWCOM Network of Excellence, a project funded from the European Commission's 6th Framework Programme (http://new.ismb.it).

II. System Model

The transmit signal of the user of interest takes the following form [10], [12]:

$$x(t) = \sum_{i=-\infty}^{+\infty} d_i f(t - iN_f T_f)$$

with

$$f(t) = \sum_{j=0}^{N_c N_f - 1} c(j) w(t - jT_c)$$

and where N_c is the number of chips of duration T_c, N_f is the number of frames of duration $T_f = N_c T_c$, $w(t)$ is the pulse of duration $T_w \ll T_c$. The transmit symbols d_i belong to a PAM format. The user code $\{c(j)\}_{j=0}^{N_c N_f - 1}$ represents either the so-called developed code in the context of Time-Hopping scheme (see, e.g., [12], [9]) or the usual code on the context of Direct Sequence scheme.

For sake of simplicity, we can consider here the single user case and the noiseless case. The transmit signal propagates through a multipath channel composed by N_p paths of magnitude $\{A_\ell\}_{\ell=1}^{N_p}$ and delay $\{\tau_\ell\}_{\ell=1}^{N_p}$. The channel is assumed to be known at the receiver side.

At the receiver, we consider a Rake receiver that selects any subset $\mathcal{L}$ of L_r paths (with $L_r \leq N_p$). When $\mathcal{L}$ contains all the paths, we get a so-called *full* Rake receiver. On the contrary, we only get a *partial* Rake receiver. Without loss of generality, the receiver demodulates the symbol d_0. In noiseless case, the continuous-time receive signal $r(t)$ takes the following form

$$y(t) = \sum_{\ell=1}^{N_p} A_\ell x(t - \tau_\ell)$$

which can be written as

$$y(t) = \sum_{i=-\infty}^{+\infty} d_i g(t - iN_f T_f)$$

with

$$g(t) = \sum_{\ell=1}^{N_p} A_\ell f(t - \tau_\ell).$$

Then, the signal at the output of the Rake receiver, denoted by z, corresponds to the projection of the received signal into the space spanned by the mapping $t \mapsto g^{(\mathcal{L})}(t)$ where

$$g^{(\mathcal{L})}(t) = \sum_{\ell \in \mathcal{L}} A_\ell f(t - \tau_\ell).$$

Therefore z can be obtained as follows

$$z =< y(t) | g^{(\mathcal{L})}(t) >$$

where $< .|. >$ stands for the inner product defined as $< f_1(t)|f_2(t) >= \int f_1(t) f_2(t) \mathrm{d}t$. Consequently, z can be expressed as follows

$$z = \sum_{\ell \in \mathcal{L}} A_\ell \int_0^{N_f T_f} y(t + \tau_\ell) f(t) \mathrm{d}t,$$

and $f(t)$ plays the role of the signal template. One can remark that the signal at the output of any Rake receiver can be split into two terms $z = z_1 + z_2$ where

$$z_1 = H d_0$$

with

$$H = N_f r(0) \sum_{\ell \in \mathcal{L}} A_\ell^2,$$

and

$$\begin{aligned} z_2 &= \sum_{\ell \in \mathcal{L}} \sum_{\substack{k=1 \\ k \neq \ell}}^{N_p} A_\ell A_k \\ &\times \left[d_{-Q_{k,\ell}} [\mathcal{C}(q_{k,\ell}) r(\varepsilon_{k,\ell}) + \mathcal{C}(q_{k,\ell} + 1) \tilde{r}(\varepsilon_{k,\ell})] \right. \\ &+ \left. d_{-Q_{k,\ell}-1} [\mathcal{D}(q_{k,\ell}) r(\varepsilon_{k,\ell}) + \mathcal{D}(q_{k,\ell} + 1) \tilde{r}(\varepsilon_{k,\ell})] \right], \end{aligned}$$

with

$$r(s) = \int_{-\infty}^{+\infty} w(t) w(t - s) dt, \quad \tilde{r}(s) = r(s - T_c),$$

and

$$\mathcal{C}(q) = \sum_{k=q}^{N_c N_f - 1} c(k) c(k - q), \quad \mathcal{D}(q) = \sum_{k=0}^{q-1} c(k) c(k - q),$$

and where $\tau_k - \tau_\ell$ can be decomposed, via an Euclidian division, as $Q_{k,\ell} N_f T_f + q_{k,\ell} T_c + \varepsilon_{k,\ell}$, such that $Q_{k,\ell} = \lfloor (\tau_k - \tau_\ell)/N_f T_f \rfloor$, $q_{k,\ell} = \lfloor ((\tau_k - \tau_\ell) - Q_{k,\ell} N_f T_f)/T_c \rfloor$, and the remainder $\varepsilon_{k,\ell} \in [0, T_c)$.

Actually, z_1 is the useful signal, and z_2 is the so-called interference [10], [9]. In [9], it has been remarked that, even in presence of large guard time interval, the variance of the interference term z_2 does not vanish. This residual interference is due to collision between pulses only shifted by a delay belonging to $[-T_w, T_w]$. As a consequence, the error probability does not tend towards zero when Signal-to-Noise Ratio increases.

III. IMPROVED RAKE RECEIVER

The interference term z_2 is viewed as nuisance term by the Rake receiver. Indeed, the term z_2 can be either positive or negative and so may bring closer the term z to the decision border. Thanks to the guard time interval, we are able to remove the inter-frame and inter-symbol interference part. But the term z_2 is still non null since it also depends on the symbol of interest d_0. This remaining term disturbs the standard Rake receiver. It is clear that this term provides useful information about the symbol of interest. Therefore, in the sequel, we will slightly modify the Rake receiver in order to take advantage of the remaining term. Firstly, we need to express the interference term z_2 into two parts

$$z_2 = H' d_0 + \tilde{z}_2$$

where

$$\begin{aligned} H' &= \sum_{\ell \in \mathcal{L}} \sum_{\substack{k=1 \\ k \neq \ell}}^{N_p} A_\ell A_k \\ &\times \left[\mathbf{1}_{Q_{k,\ell}=0} [\mathcal{C}(q_{k,\ell}) r(\varepsilon_{k,\ell}) + \mathcal{C}(q_{k,\ell} + 1) \tilde{r}(\varepsilon_{k,\ell})] \right. \\ &+ \left. \mathbf{1}_{Q_{k,\ell}=-1} [\mathcal{D}(q_{k,\ell}) r(\varepsilon_{k,\ell}) + \mathcal{D}(q_{k,\ell} + 1) \tilde{r}(\varepsilon_{k,\ell})] \right] \end{aligned}$$

and $\mathbf{1}_X$ is equal to one if X is right, and to zero otherwise.

The receive signal thus can be written as follows

$$z = \tilde{z}_1 + \tilde{z}_2$$

with

$$\tilde{z}_1 = (H + H') d_0. \tag{1}$$

where $\tilde{z}_1$ contains the information about the symbol of interest coming from the useful term z_1 and the "nuisance" term z_2, and where $\tilde{z}_2$ only contains the inter-symbol interference. Therefore, when only the residual interference occurs (*i.e.*, $H' d_0$), the term $\tilde{z}_2$ is null.

When partial Rake receiver is used, $H + H'$ may be negative which gives rise to error detection. Notice that when full Rake receiver is applied (which is unrealistic in practice), $H + H'$ is positive, by construction, whatever the channel realization. Indeed, in absence of inter-symbol interference, we get

$$z = d_0 < g(t) | g^{(\mathcal{L})}(t) >$$

and by comparing this previous equation with Eq. (1), we have $H + H' =< g(t) | g^{(\mathcal{L})}(t) >$. For full Rake receiver, as $g(t) = g^{(\mathcal{L})}(t)$, the term $H + H$ is equal to a squared norm and is thus strictly positive. On the contrary, for partial Rake receiver, $g(t)$ is different from $g^{(\mathcal{L})}(t)$ and we can not conclude.

To counter-act the possible negative term $H + H'$, we need to carry out a one-tap filter equalization. Therefore, in the context of binary PAM (which is the most likely), it is enough to multiply z by $H + H'$. Then we will take the final decision on z' built as follows

$$z' = (H + H') z = (H + H')^2 d_0 + (H + H') \tilde{z}_2.$$

We observe that, in absence of inter-symbol interference ($\tilde{z}_2 = 0$), z' is always in the right decision region.

For multi-level PAM, z' may be deduced from z by applying a one-tap Wiener filter (for instance, $z' = Wz$ with $W = (H+H')/((H+H')^2+\sigma^2)$ and σ^2 the noise variance).

Finally Figure 1 describes the improved Rake receiver where the dot lines corresponds to the proposed extra operations.

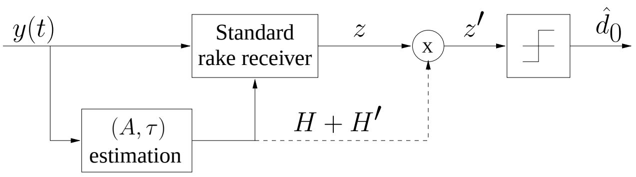

Fig. 1. Improved Rake receiver principle

In order to carry out the standard Rake receiver, we need to estimate the amplitude and the delay of each path belonging to the set $\mathcal{L}$. To compute the improved Rake receiver, we additionally need to have the knowledge of $(H+H')$. Although $(H+H')$ depends on the amplitude and delay of all the paths, we fortunately do not have to estimate all the components of the multipath channel. Indeed, by using Eq. (1), we remark that stimating $(H+H')$ is an easy task if a training sequence[2] is available. Consequently, the extra computational load is negligible compared to the standard Rake receiver.

IV. Simulations

We consider $T_f = 50$ ns, $T_c = 5$ ns, $N_f = 3$, $N_c = 10$, and $T_w = 1$ ns. The symbol period is thus equal to 150 ns. As a 2-PAM is employed, the data rate is 6.6 Mbs/s. The previous set-up is usual for the IEEE 802.13.4a standard associated with medium data rate and long range applications. Parameters of the Gaussian pulse $w(t)$ are chosen such that the pulse spectrum fits the shape of the FCC spectral mask [13]. For practical purpose, the pulse (with unitary energy) is truncated to duration $T_w = 1$ ns, and thus, can be written as:

$$w(t) = \frac{2\sqrt{2}}{\sigma_w^2 \pi}\cos(2\pi f_0(t - T_w/2))e^{-(t-T_w/2)^2/2\sigma_w^2} \times \mathbf{1}_{[0,T_w]}$$

with $\sigma_w^2 = 911 \times 10^{-4}$ ns and $f_0 = 6.85$ GHz.

The statistical channel model considered hereafter is the conventional one established for UWB personal area network [14], [15] with one cluster only. In [16], it has been shown that considering one cluster instead of several clusters was not restrictive and obviously much simpler. We remind that the amplitudes are zero-mean random variables given by $A_\ell = a_\ell \cdot e^{-\tau_\ell/2\gamma}$ with γ the ray decay factor, and $a_\ell = p_\ell \cdot \beta_\ell$ where $p_\ell \in \{-1,+1\}$ is an equi-likely binary random sequence and where β_ℓ is a log-normal random variable. The delays τ_ℓ are independent Poisson random variables with parameter λ and as a consequence, the difference between two consecutive delays obeys an exponential distribution with parameter λ. Consequently λ represents the path "density". In Appendix, we prove that γ (in the context of an unique cluster) is the delay spread of the channel. As a consequence γ refers to as the channel "length".

[2]also sent for estimating the amplitude and the delay of each path belonging to the set $\mathcal{L}$

Like [17], we compute the true average error probability at the output of the Rake receiver. It is given by $P_e(a,\tau,d) = \Pr\{z < 0|a,\tau,d\}$ assuming that the transmitted symbol d_0 is fixed and is equal to 1. The average error probability denoted $\bar{P}_e$ is then obtained by averaging $P_e(a,\tau,d)$ over all the random variables and can be written $\bar{P}_e = \mathbb{E}_{a,\tau,d^*}[\Pr\{z < 0|a,\tau,d\}]$ where $d^* = d/\{d_0\}$. As the noise is zero-mean Gaussian, $\bar{P}_e$ reduces as follows:

$$\bar{P}_e = \mathbb{E}_{a,\tau,d^*}\left[\frac{1}{2}\text{erfc}\left(\frac{z_1+z_2}{\sqrt{2}\ \sigma}\right)\right]$$

where σ^2 is the variance of the filtered Gaussian noise at the output of the Rake receiver. Given a realization of the channel, we get

$$\sigma^2 = \frac{N_0}{2}N_f r(0)\sum_{\ell,\ell' \in \mathcal{L}} A_\ell A_{\ell'}$$

where $N_0/2$ is the variance of the continuous-time white Gaussian noise $n(t)$ encountered in the propagation environment.

We also define the average Signal-to-Noise Ratio denoted by $\bar{E}_b/N_0$ where $\bar{E}_b = \mathbb{E}_{a,\tau,d}[\int_0^{N_f T_f} y^2(t)dt]$ stands for the average receive energy per bit. For our channel model, we find

$$\bar{E}_b = N_f r(0)\sum_{\ell=1}^{N_p} \lambda^\ell (\lambda + 1/\gamma)^{-\ell}.$$

The number of fingers of the Rake receiver is fixed to $L_r = 1$. Similar results could be obtained with a larger number of fingers.

At each trial, the user code and the channel realization are changed. We average the error probability over 1000 runs.

On Figures 2, 3, 4, and 5, we plot $\bar{P}_e$ versus $\bar{E}_b/N_0$ for the standard and improved Rake receivers in the case of channels CM1, CM2, CM3, and CM4 with one cluster respectively. For exemple, in the context of CM3, the delay spread is 7.9 ns, and thus it gives rise to a lot of residual interference but to little inter-symbol interference. We observe that the gain in performance is substantial.

On Figure 6, we display $\bar{P}_e$ versus γ the so-called delay spread for both receivers when path density remains constant and equal to $\lambda = 2\text{ns}^{-1}$ and when $\bar{E}_b/N_0 = 30$dB. We remark that the gain can be neglected when the delay spread becomes close to the symbol period, that is to say that, when true inter-symbol interference occurs.

On Figure 7, we display $\bar{P}_e$ versus λ the so-called path density for both receivers when delay spread remains constant and equal to $\gamma = 5$ns and when $\bar{E}_b/N_0 = 30$dB. We remark that the gain is almost independent of the path density.

V. Conclusion

In order to handle properly the residual interference, we have introduced an improved version of the Rake receiver with minor extra complexity in the context of PAM Time-Hopping/Direct Sequence Impulse Radio Ultra Wide Band.

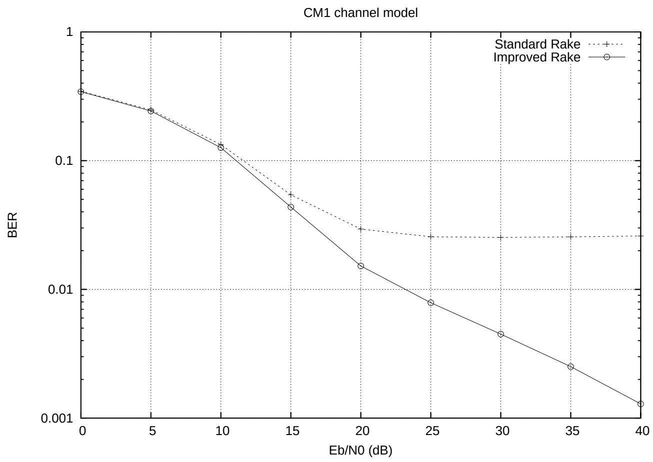

Fig. 2. Average error probability vs. "signal-to-noise ratio" for CM1

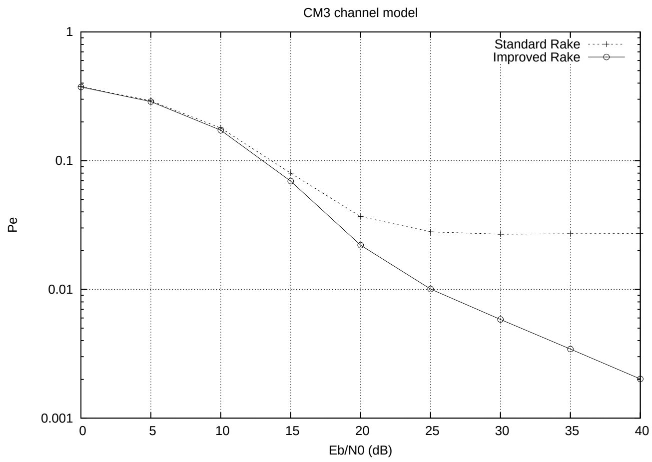

Fig. 4. Average error probability vs. "signal-to-noise ratio" for CM3

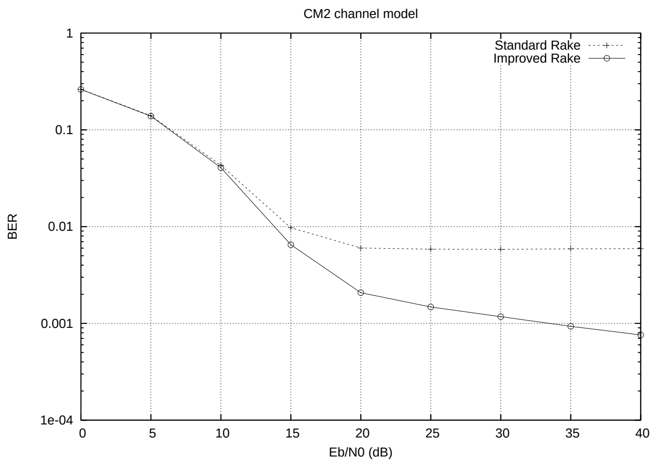

Fig. 3. Average error probability vs. "signal-to-noise ratio" for CM2

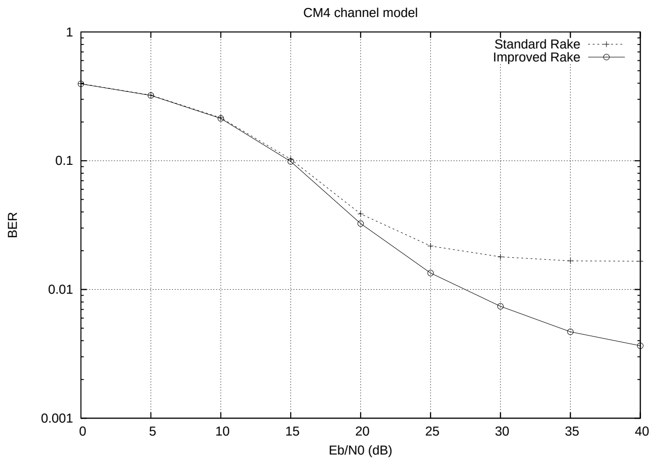

Fig. 5. Average error probability vs. "signal-to-noise ratio" for CM4

APPENDIX

First of all, we need to evaluate the path probability density function.

Since we only consider one cluster, we know that the difference between two consecutive delays $\tau_{\ell-1}$ and τ_ℓ, denoted by t_ℓ, is a random variable satisfying an exponential distribution $t \mapsto p_t(t)$ with parameter λ. Moreover the random process t_ℓ is independent and identically distributed. As $\tau_\ell = \sum_{k=1}^{\ell} t_k$, we get

$$p_{\tau_\ell}(t) = \underbrace{p_t(t) \star p_t(t) \star \cdots \star p_t(t)}_{\ell \text{ times}}$$

where $\star$ stands for the convolutive product and where p_t is the distribution of t. One can then easily check that

$$p_{\tau_\ell}(t) = \frac{\lambda^\ell}{(\ell-1)!} t^{\ell-1} e^{-\lambda t} \mathbf{1}_{t \geq 0} \tag{2}$$

where $\mathbf{1}_{t\geq 0}$ is equal to 1 if t is positive and zero otherwise.

In order to determine the Mean Excess Delay and the Root Mean Square Delay Spread [18], [19], we have to derive the Power Delay Profile $P(t)$ defined as follows

$$P(t) = \mathbb{E}[|h(t)|^2]$$

where

$$h(t) = \sum_{\ell=1}^{N_p} A_\ell \delta(t - \tau_\ell).$$

As $A_\ell = a_\ell e^{-\tau_\ell/2\gamma}$ and as a_ℓ is independent of τ_ℓ, we obtain that

$$\mathbb{E}[|h(t)|^2] = \sum_{\ell,\ell'=1}^{N_p} \mathbb{E}[a_\ell a_{\ell'}] \mathbb{E}[e^{-(\tau_\ell+\tau_{\ell'})/2\gamma} \delta(t-\tau_\ell)\delta(t-\tau_{\ell'})].$$

Since a_ℓ are independent and identically distributed (with variance Ω_0), one can write

$$\mathbb{E}[|h(t)|^2] = \sum_{\ell=1}^{N_p} \Omega_0 \mathbb{E}[e^{-\tau_\ell/\gamma} \delta(t-\tau_\ell)].$$

Therefore

$$\mathbb{E}[|h(t)|^2] = \Omega_0 \sum_{\ell=1}^{N_p} \int e^{-\tau_\ell/\gamma} \delta(t-\tau_\ell) p_{\tau_\ell}(\tau_\ell) d\tau_\ell$$

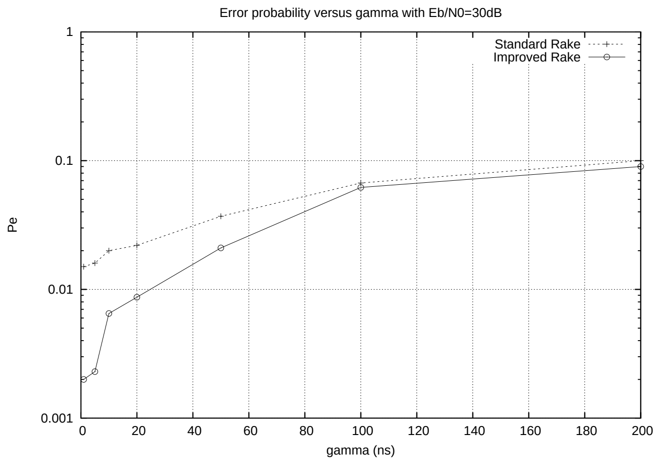

Fig. 6. Average error probability vs. ”delay spread”

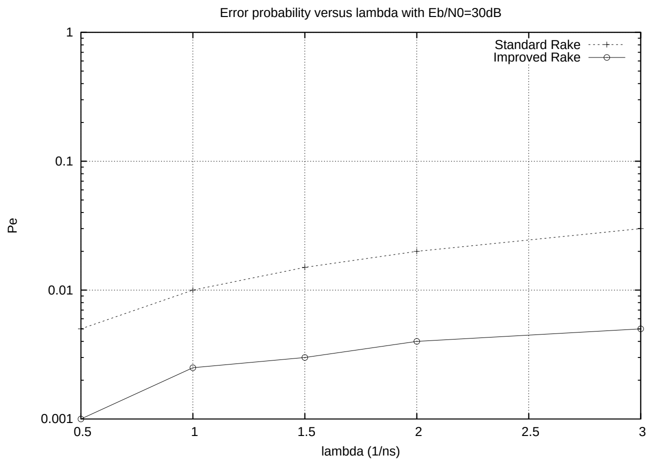

Fig. 7. Average error probability vs. ”path density”

and then

$$\mathbb{E}[|h(t)|^2] = \Omega_0 \sum_{\ell=1}^{N_p} e^{-t/\gamma} p_{\tau_\ell}(t).$$

By using Eq. (2) and by considering that N_p is large, we finally obtain

$$P(t) = \Omega_0 \lambda e^{-t/\gamma}.$$

The normalized power delay profile $\tilde{P}(t)$ such that $\int \tilde{P}(t)dt = 1$ can be introduced as follows

$$\tilde{P}(t) = \frac{1}{\gamma} e^{-t/\gamma}.$$

The normalized profile can play the role of the ”probability density” and actually exhibits the mean power located at time t. Consequently, it is relevant to define the Mean Excess Delay as

$$t_{\rm m} = \mathbb{E}[t] = \int_0^{+\infty} t\tilde{P}(t)dt$$

when t is $\tilde{P}(t)$-distributed. After straightforward algebraic manipulations, we get

$$t_{\rm m} = \gamma.$$

Then the Root Mean Square Delay Spread (around the Mean Excess Delay) can be defined as follows

$$t_{\rm rms} = \sqrt{\mathbb{E}[(t - t_{\rm m})^2]} = \sqrt{\int_0^{+\infty} (t - t_{\rm m})^2 \tilde{P}(t)dt}.$$

One can easily check that

$$t_{\rm rms} = \gamma$$

which concludes the proof.

REFERENCES

[1] M.E. Sahin, H. Arslan, ”Inter-Symbol inerference in high data rate UWB communications using energy detector receivers”, *IEEE Int. Conf. on UltraWide Band (ICU)*, Sep. 2005.

[2] A. Parihar, *et al.*, ”Analysis of Equalization for DS-UWB systems”, *IEEE Int. Conf. on UltraWide Band (ICU)*, Sep. 2005.

[3] Y. Li, A. Molisch, ”Channel Estimation and Signal Detection for UWB”, *Int. Symp. on WPMC*, 2003.

[4] L. Zhiwei, A.B. Premkumar, A.S. Madhukumar, ”Matching Pursuit-based tap selection technique for UWB channel equalization”, *IEEE Communications Letters*, Sep. 2005.

[5] M. Eslami, X. Dong, ” Rake-MMSE-Equalizer performance for UWB”, *IEEE Communications Letters*, June 2005.

[6] H. Celebi, H. Arslan, ”Cross-Modulation Interference for Pulse Position modulated UWB signals”, *IEEE Int. Conf. on Military Communications (MILCOM)*, Nov. 2005.

[7] K. Usuda, H. Zhang, M. Nakagawa, ”M-ary pulse shape modulation for PSWF-based UWB systems in multipath fading environment”, *IEEE Int. Conf. on Global Communications (GLOBECOM)*, Nov. 2004.

[8] S. Zhao, H. Liu, ”On the optimum linear receiver for impulse radio systems on the presence of pulse overlapping ”, *IEEE Communications Letters*, April 2005.

[9] A.-L. Deleuze, P. Ciblat, C. Le Martret, ”Inter-Symbol/Inter-Frame Interference in Time-Hopping Ultra Wideband Impulse Radio system”, *IEEE Int. Conf. on Ultra-Wideband (ICU)*, Sep. 2005.

[10] M. Z. Win, R. A. Scholtz, “Ultra-wide bandwidth time-hopping spread-spectrum impulse radio for wireless multiple-access communications,” *IEEE Trans. on Communications*, vol. 48, no. 4, April 2000.

[11] F. Ramírez-Mireles, “Error probability of ultra wideband SSMA in a dense multipath environment,” in *Proc. of the Milcom Conf.* , vol. 2, Anaheim, CA, USA, pp. 1081-1084, Oct. 2002.

[12] C. Le Martret, G. B. Giannakis, “All-Digital impulse radio for wireless cellular systems,” *IEEE Trans. on Communications*, vol. 50, no. 9, pp. 1440-1450, Sept. 2002.

[13] Federal Communication Commission, “Revision of Part 15 of the commission’s rules regarding ultra-wideband transmission systems, first Report and Order,” FCC, Feb. 2002.

[14] A.A.M. Saleh, R. A. Valenzuela, “A statistical model for indoor multipath propagation,” *Journal of Selected Areas in Comm.*, vol. 5, pp. 128-137, Feb. 1987.

[15] A. F. Molish, J. R. Foerster, M. Pendergrass, “Channel models for ultrawideband personal area networks,” *IEEE Wireless Communications*, vol. 10, Dec. 2003.

[16] R. D. Wilson, R. A. Scholtz, “Comparison of CDMA and modulation schemes for UWB radio in a multipath environment,” in *Proc. of IEEE Global Telecomm. Conf. (GLOBECOM)*, vol. 2, pp. 754-758, Dec. 2003.

[17] G. Durisi, S. Benedetto, “Performance evaluation of TH-PPM UWB systems in the presence of multiuser interference,” *IEEE Communications Letters*, May 2003.

[18] A. F. Molisch, ”Statistical properties of the RMS delay spread of mobile radio channels with independent rayleigh-fading paths,” *IEEE Trans. on Vehicular Technology*, vol. 45, pp. 201-204, Feb. 1996.

[19] M. Sánchez Varela and M.G. Sánchez, ”RMS delay and coherence bandwidth measurements in indoor radio channels in the UHF band,” *IEEE Trans. on Vehicular Technology*, vol. 50, pp. 515-525, Mar. 2001.